

# Developed mathematical technique for fractional stochastic point kinetics model in nuclear reactor dynamics

Ahmed E. Aboanber<sup>2</sup> · Abdallah A. Nahla<sup>1,2</sup> · Adel M. Edress<sup>2</sup>

Received: 16 September 2017 / Revised: 10 March 2018 / Accepted: 29 March 2018 / Published online: 27 July 2018

© Shanghai Institute of Applied Physics, Chinese Academy of Sciences, Chinese Nuclear Society, Science Press China and Springer Nature Singapore Pte Ltd. 2018

**Abstract** Fractional stochastic kinetics equations have proven to be valuable tools for the point reactor kinetics model, where the nuclear reactions are not fully described by deterministic relations. A fractional stochastic model for the point kinetics system with multi-group of precursors, including the effect of temperature feedback, has been developed and analyzed. A major mathematical and inflexible scheme to the point kinetics model is obtained by merging the fractional and stochastic technique. A novel split-step method including mathematical tools of the Laplace transforms, Mittag-Leffler function, eigenvalues of the coefficient matrix, and its corresponding eigenvectors have been used for the fractional stochastic matrix differential equation. The validity of the proposed technique has been demonstrated via calculations of the mean and standard deviation of neutrons and precursor populations for various reactivities: step, ramp, sinusoidal, and temperature reactivity feedback. The results of the proposed method agree well with the conventional one of the deterministic point kinetics equations.

**Keywords** Itô stochastic point kinetics equations · Temperature feedback effects · Wiener process · Fractional calculus · Mittag-Leffler function

## 1 Introduction

The dynamical processes described by the linear or nonlinear point kinetics equations are random processes in nature, that is, due to the neutron population and precursor concentrations of delayed neutrons varying randomly with time. At the levels of high power, the stochastic manner is imperceptible, while at low-power levels, for example, at the start-up of reactor operation, random fluctuation in the neutron population density and neutron precursor concentrations can be useful. The behavior variations of neutron population and precursor concentrations for nuclear reactors have been described by several innovators through employing stochastic models. Hayes and Allen [1] are the first authors who derived the stochastic model of the linear point reactor kinetics equations. They introduced a simplified stochastic model based on the Itô stochastic differential equations. The numerical results of this model using stochastic piecewise constant approximation (SPCA) have been compared with the Monte Carlo (MC) calculations and the experimental measurements [2]. Ha and Kim [3, 4] have presented the stochastic space-dependent kinetics model (SSKM) to solve the one-dimensional monoenergetic space-time reactor kinetics. In 2012, Ray [5] developed Taylor 1.5 strong order methods and the Euler–Maruyama to solve the stochastic point kinetics equations with step reactivity, while in 2013, Ray and Patra [6] presented the same techniques with sinusoidal reactivity. The stochastic partial differential equation and stochastic

---

✉ Abdallah A. Nahla  
a.nahla@science.tanta.edu.eg

Ahmed E. Aboanber  
ahmed.aboanber@science.tanta.edu.eg

Adel M. Edress  
adel.edress@science.tanta.edu.eg

<sup>1</sup> Department of Mathematics, Faculty of Science, Taibah University, Al-Madinah 41411, Saudi Arabia

<sup>2</sup> Department of Mathematics, Faculty of Science, Tanta University, Tanta 31527, Egypt

difference equations have been presented by Ref. [7] for neutron transport equation. Furthermore, the power doubling time for a subcritical reactor is identified through the point kinetics system by Allen as a stochastic first-passage time problem [8]. In 2013, Ray and Patra [9] were the first authors who presented a numerical solution of fractional stochastic neutron point kinetic equations. Ayyoubzadeh and Vosoughi [10] simplified the system of Itô stochastic differential equations via alternative derivation of the stochastic differential equations. In 2016, Nahla and Edress [11] utilized the analytical exponential model (AEM) for the simplest formula of the stochastic point reactor kinetics system with various reactivities. They also proposed an efficient stochastic model (ESM) for the point kinetics model in Ref. [12]. da Silva et al. [13] presented a solution for the stochastic neutron point kinetics model. In 2017, Nahla [14] developed the analytical exponential technique (AET) to solve a stochastic nonlinear system of the point reactor kinetics equations with Newtonian temperature feedback reactivity. Finally, Singh and Ray [15] presented a comparison of two split-step methods for the numerical simulation of stochastic point kinetics equations in the presence of Newtonian temperature feedback effects.

The fundamental objective of this work is speculation of the stochastic point kinetics system to a fractional stochastic point kinetics system including multi-group of the precursor concentration. To overcome the difficulty arising from the merging of the fractional and stochastic techniques, a developed mathematical technique is presented for solving the equation in the matrix form of the proposed fractional stochastic model. This technique is based on split-step technique, Laplace transforms, the Mittag-Leffler function, eigenvalues of the coefficient matrix, and its corresponding eigenvectors. The proposed method is applied to the fractional stochastic point kinetics system with various reactivities and different fractional orders.

The paper is sorted out as follows: The preliminaries of the stochastic model, as well as the definitions of the Wiener process and fractional calculus, are introduced in Sect. 2. The solution of the fractional stochastic point kinetics equations with multi-group of a delayed precursor is derived in Sect. 3. The computational numerical results of the proposed system are discussed and compared with various stochastic techniques in Sect. 4. General conclusions including future work are presented in Sect. 5.

## 2 Preliminaries

In the following subsections, preliminaries of the Itô stochastic model, Wiener process, and fractional calculus are introduced briefly.

### 2.1 Itô stochastic model

Let us consider the following Itô stochastic differential model: [16]

$$d\mathbf{X}(t) = g(t, \mathbf{X}(t))dt + f(t, \mathbf{X}(t))d\mathbf{W}(t), \quad (1)$$

where  $g : \mathbb{R}^+ \times \mathbb{R}^m \rightarrow \mathbb{R}^m$  and  $f : \mathbb{R}^+ \times \mathbb{R}^m \rightarrow \mathbb{R}^{m \times m}$  are locally bounded and measurable functions and  $\mathbf{W}(t)$  is an  $m$ -dimensional Wiener process which is defined as the diffusion term.

The general solution of Eq. (1) can be written as:

$$\begin{aligned} \mathbf{X}(t) = \mathbf{X}(0) &+ \int_0^t g(u, \mathbf{X}(u))du \\ &+ \int_0^t f(u, \mathbf{X}(u))d\mathbf{W}(u). \end{aligned} \quad (2)$$

Here, the integral  $\int_0^t g(u, \mathbf{X}(u))du$  is typically the Riemann–Lebesgue integral, while the integral  $\int_0^t f(u, \mathbf{X}(u))d\mathbf{W}(u)$  is considered as an Itô integral. Generally, the analytical solution of the multi-dimensional Eq. (2) to a great or significant extent is not possible, and numerical techniques are robustly utilized.

### 2.2 Wiener process

Recall that the standard Wiener process is a continuous-time stochastic process which is also called the standard Brownian motion. The Wiener process  $W(t)$  over  $[0, T]$  is a random variable,  $W(t)$ , that depends on a continuous time,  $t$ , and is characterized by three conditions as follows [17]:

1.  $W(t) = 0$  for  $t = 0$
2.  $W(t)$  has independent increments with  $W(t) - W(s) \sim \sqrt{t-s}\mathcal{N}(0, 1)$  for  $s \in [0, t]$ , where  $\mathcal{N}(0, 1)$  is the normal distribution with zero mean and unit variance.
3. For  $0 \leq s_1 < t_1 < s_2 < t_2 \leq T$ , the increments  $W(t_1) - W(s_1)$  and  $W(t_2) - W(s_2)$  are independent random variables.

For numerical computational object, it is helpful to assume the discretized Brownian motion, where  $W(t)$  is specialized at discrete values,  $t$ . Accordingly, for some positive integer,  $N$ , consider  $h = T/N$  and let  $W_i$  denote  $W(t_i)$  with  $t_i = ih$ . The first condition states that  $W_0 = 0$  with the probability equal to one and the other conditions state that  $W_i = W_{i-1} + dW_i$ ,  $i = 1, 2, \dots, N$ , where each  $dW_i$  is an independent random variable of the form  $\sqrt{h}\mathcal{N}(0, 1)$ .

### 2.3 Fractional calculus

The Riemann–Liouville fractional integral and Caputo derivative are defined, respectively, as follows:

**Definition 1** [18] Let  $g(t)$  be a continuous function,  $\alpha \geq 0$  and  $t \in R$ . The Riemann–Liouville integral can be defined as:

$$I_x^\alpha g(x) = \frac{1}{\Gamma(\alpha)} \int_0^x (x-t)^{\alpha-1} g(t) dt, \tag{3}$$

where  $\Gamma(\alpha)$  is the gamma function of the fractional order.

**Definition 2** [19] Let  $n$  be an integer number, where  $n - 1 < \alpha < n$  and  $x > 0$ . The Caputo fractional derivative of order  $\alpha$  for a function  $g(x)$  is defined as

$$D_x^\alpha g(x) = \frac{1}{\Gamma(n-\alpha)} \int_0^x (x-t)^{n-\alpha-1} g^{(n)}(t) dt, \tag{4}$$

where  $g^{(n)}(t) = \frac{\partial^n g(t)}{\partial t^n}$ .

The relation between the Caputo fractional derivative [20] and the Riemann–Liouville fractional integral is introduced in the following formula:

$$I_x^\alpha D_x^\alpha g(x) = g(x) - \sum_{r=0}^{n-1} g^{(r)}(0_+) \frac{x^r}{r!}, \quad n-1 < \alpha \leq n. \tag{5}$$

### 3 Developed mathematical technique

The fractional stochastic model of the point reactor kinetics equation can be written as: [1, 2, 21, 22]

$$D_t^\alpha |\mathbf{P}(t)\rangle = \mathbf{A}|\mathbf{P}(t)\rangle + |\mathbf{Q}\rangle + \mathbf{B}^{\frac{1}{2}} D_t |\mathbf{W}(t)\rangle, \tag{6}$$

where

$$|\mathbf{P}(t)\rangle = \begin{pmatrix} n(t) \\ c_1(t) \\ c_2(t) \\ \vdots \\ c_I(t) \end{pmatrix}, \tag{7}$$

$$\mathbf{A} = \begin{pmatrix} \frac{\rho - \beta}{\Lambda} & \lambda_1 & \lambda_2 & \cdots & \lambda_I \\ \frac{\beta_1}{\Lambda} & -\lambda_1 & 0 & \cdots & 0 \\ \frac{\beta_2}{\Lambda} & 0 & -\lambda_2 & \cdots & 0 \\ \vdots & \vdots & \ddots & \ddots & \vdots \\ \frac{\beta_I}{\Lambda} & 0 & \cdots & 0 & -\lambda_I \end{pmatrix},$$

$$|\mathbf{Q}\rangle = \begin{pmatrix} q \\ 0 \\ 0 \\ \vdots \\ 0 \end{pmatrix},$$

$t$  is the time,  $n(t)$  is the neutron population,  $\rho$  is the total reactivity,  $c_i(t)$  is the  $i$ -group of delayed precursor

concentration,  $\lambda_i$  is the decay constant of  $i$ -group of delayed neutrons,  $\beta_i$  is the fraction of  $i$ -group delayed neutrons,  $\beta = \sum_{i=1}^I \beta_i$  is the total fraction of delayed neutrons,  $I$  is the total number of delayed neutron groups,  $\Lambda$  is the prompt neutron generation time,  $q$  is the external source of neutrons,

$$|\mathbf{W}(t)\rangle = \begin{pmatrix} W_1(t) \\ W_2(t) \\ W_3(t) \\ \vdots \\ W_{I+1}(t) \end{pmatrix},$$

$$\mathbf{B} = \begin{pmatrix} \left(\frac{\rho + \beta}{\Lambda}\right)n - \sum_{i=1}^I \lambda_i c_i + q & -\frac{\beta_1}{\Lambda}n + \lambda_1 c_1 & -\frac{\beta_2}{\Lambda}n + \lambda_2 c_2 & \cdots & -\frac{\beta_I}{\Lambda}n + \lambda_I c_I \\ -\frac{\beta_1}{\Lambda}n + \lambda_1 c_1 & \frac{\beta_1}{\Lambda}n - \lambda_1 c_1 & 0 & \cdots & 0 \\ -\frac{\beta_2}{\Lambda}n + \lambda_2 c_2 & 0 & \frac{\beta_2}{\Lambda}n - \lambda_2 c_2 & \cdots & 0 \\ \vdots & \vdots & \ddots & \ddots & \vdots \\ -\frac{\beta_I}{\Lambda}n + \lambda_I c_I & 0 & \cdots & 0 & \frac{\beta_I}{\Lambda}n - \lambda_I c_I \end{pmatrix}, \tag{8}$$

and  $|\Delta \mathbf{W}(t)\rangle = \sqrt{h}|\eta\rangle$  such that  $W_1(t), W_2(t), \dots, W_{I+1}(t)$  are the Wiener processes [5, 17].

Notice that the initial condition can be determined as  $n(0) = n_0$ ,  $\frac{dn(t)}{dt}|_{t=0} = 0$ , and  $\frac{dc_i(t)}{dt}|_{t=0} = 0, i = 1, 2, \dots, I$ . This means that

$$|\mathbf{P}(0)\rangle = \begin{pmatrix} n_0 \\ \frac{\beta_1 n_0}{\Lambda \lambda_1} \\ \frac{\beta_2 n_0}{\Lambda \lambda_2} \\ \vdots \\ \frac{\beta_I n_0}{\Lambda \lambda_I} \end{pmatrix}. \tag{9}$$

Of course, when the variance matrix  $\mathbf{B} = 0$  and the fractional derivative order  $\alpha = 1$ , Eq. (6) is reduced to the standard point reactor kinetics model.

In what follows, we aim to solve the fractional stochastic differential Eq. (6). The technique of split-step was utilized, that is, Eq. (6) is separated into deterministic and stochastic parts, followed by solving each of them separately. Applying the Laplace transformation on the deterministic part, i.e., consider  $\mathbf{B} = 0$ , of Eq. (6) is as follows [23–25]:

$$s^\alpha |\mathcal{P}(s)\rangle - s^{\alpha-1} |\bar{\mathbf{P}}(0)\rangle - \mathbf{A}|\mathcal{P}(s)\rangle = \frac{1}{s} |\mathbf{Q}\rangle, \tag{10}$$

where  $|\mathcal{P}(s)\rangle = \mathcal{L}[|\bar{\mathbf{P}}(t)\rangle]$ ,  $|\bar{\mathbf{P}}(t)\rangle$  is the solution of the deterministic part for Eq. (6). Consequently, we get:

$$|\mathcal{P}(s)\rangle = s^{\alpha-1}[s^\alpha \mathbf{I} - \mathbf{A}]^{-1}|\bar{\mathbf{P}}(0)\rangle + \frac{1}{s}[s^\alpha \mathbf{I} - \mathbf{A}]^{-1}|\mathbf{Q}\rangle. \tag{11}$$

Using the inverse Laplace transformation, we have:

$$|\bar{\mathbf{P}}(t)\rangle = E_{\alpha,1}(\mathbf{A}t^\alpha)|\bar{\mathbf{P}}(0)\rangle + \int_0^t (t-\tau)^{\alpha-1} E_{\alpha,\alpha}(\mathbf{A}(t-\tau)^\alpha) d\tau |\mathbf{Q}\rangle. \tag{12}$$

Let us introduce the parameter  $z = t - \tau$  into Eq. (12) to have:

$$|\bar{\mathbf{P}}(t)\rangle = E_{\alpha,1}(\mathbf{A}t^\alpha)|\bar{\mathbf{P}}(0)\rangle + \int_0^t z^{\alpha-1} E_{\alpha,\alpha}(\mathbf{A}z^\alpha) dz |\mathbf{Q}\rangle. \tag{13}$$

Using the integration property of the Mittag-Leffler function which is:

$$\int_0^t z^{b-1} E_{a,b}(\mathbf{A}z^a) dz = t^b E_{a,b+1}(\mathbf{A}t^a), \tag{14}$$

for  $b > 0$ , then Eq. (13) reads as follows:

$$|\bar{\mathbf{P}}(t)\rangle = E_{\alpha,1}(\mathbf{A}t^\alpha)|\bar{\mathbf{P}}(0)\rangle + t^\alpha E_{\alpha,\alpha+1}(\mathbf{A}t^\alpha)|\mathbf{Q}\rangle. \tag{15}$$

Equation (15) introduces the general solution of the fractional stochastic point reactor kinetics equations, which depends on the stiff coefficient matrix  $\mathbf{A}$ . To overcome the stiffness of this matrix, the coefficient matrix  $\mathbf{A}$  was changed by its eigenvalues,  $\omega_j$  [26–28], and the corresponding eigenvectors,  $|\mathbf{V}_i\rangle$ , of the matrix  $\mathbf{A}$  [29–32]. Furthermore, over a small time interval with step size  $h$ , the matrices  $\mathbf{B}$  and  $\mathbf{A}$  are considered constant over the specified time interval  $[t_m, t_{m+1}]$  where  $t_{m+1} = t_m + h$  and  $m = 0, 1, 2, \dots, M - 1$ . As a result of this substitution, the Mittag-Leffler function can be written as:

$$E_{a,b}(\mathbf{A}z^\alpha) = \sum_{j=0}^l E_{a,b}(\omega_j z^\alpha) |\mathbf{V}_j\rangle \langle \mathbf{U}_j|, \tag{16}$$

where the coefficient matrix  $\mathbf{A}$  satisfies the following property in bra-ket space [33]

$$\mathbf{A}|\mathbf{V}_j\rangle = \omega_j |\mathbf{V}_j\rangle, \quad \langle \mathbf{U}_j | \mathbf{A}^T = \langle \mathbf{U}_j | \omega_j, \tag{17}$$

and

$$\langle \mathbf{U}_l | \mathbf{V}_j \rangle = \delta_{l,j} = \begin{cases} 1, & l = j \\ 0, & l \neq j \end{cases}. \tag{18}$$

The ket eigenvector,  $|\mathbf{V}_j\rangle$ , can be written by the following analytical form [33]

$$|\mathbf{V}_j\rangle = \sigma_j \begin{pmatrix} 1 \\ \frac{\beta_1}{\Lambda(\omega_j + \lambda_1)} \\ \frac{\beta_2}{\Lambda(\omega_j + \lambda_2)} \\ \vdots \\ \frac{\beta_l}{\Lambda(\omega_j + \lambda_l)} \end{pmatrix}, \tag{19}$$

and the bra eigenvector,  $\langle \mathbf{U}_j |$ , is

$$\langle \mathbf{U}_j | = \sigma_j \left( 1 \quad \frac{\lambda_1}{(\omega_j + \lambda_1)} \quad \frac{\lambda_2}{(\omega_j + \lambda_2)} \quad \dots \quad \frac{\lambda_l}{(\omega_j + \lambda_l)} \right). \tag{20}$$

From the normalization  $\langle \mathbf{U}_j | \mathbf{V}_j \rangle = 1$ , we can deduce:

$$\sigma_j = \left( 1 + \sum_{i=1}^l \frac{\beta_i \lambda_i}{\Lambda(\omega_j + \lambda_i)^2} \right)^{-\frac{1}{2}}, \quad \forall j = 0, 1, 2, \dots, l. \tag{21}$$

After introducing Eq. (16) into Eq. (15), we get:

$$|\bar{\mathbf{P}}(t_{m+1})\rangle = \sum_{j=0}^l [E_{\alpha,1}(\omega_j h^\alpha) |\mathbf{V}_j\rangle \langle \mathbf{U}_j | \bar{\mathbf{P}}(t_m)\rangle + h^\alpha E_{\alpha,\alpha+1}(\omega_j h^\alpha) |\mathbf{V}_j\rangle \langle \mathbf{U}_j | \mathbf{Q}\rangle]. \tag{22}$$

The obtained results,  $|\bar{\mathbf{P}}(t_{m+1})\rangle$ , from Eq. (22), were used to evaluate the variance matrix  $\bar{\mathbf{B}}(t_{m+1})$ . Furthermore, according to the split-step method, the general solution of Eq. (6) is given by:

$$|\mathbf{P}(t_{m+1})\rangle = |\bar{\mathbf{P}}(t_{m+1})\rangle + \sqrt{h} \bar{\mathbf{B}}^{\frac{1}{2}}(t_{m+1}) |\eta\rangle, \tag{23}$$

where  $|\Delta \mathbf{W}(t)\rangle = \sqrt{h} |\eta\rangle$ .

Equation (23) represents the general solution of the fractional stochastic point kinetics model with a multi-group of delayed precursor concentration.

### 4 Computational results

In order to affirm the exactness and validity of the proposed technique over the traditional methods, the developed mathematical technique (DMT) for the fractional stochastic point kinetics model with a multi-group of delayed precursor concentration is tested through Matlab code. The mean and standard deviation of the neutron populations and precursor concentrations in different cases of reactivities, step, ramp, sinusoidal, and also in the presence of temperature feedback, are calculated. The results of the proposed method are compared to five

**Table 1** Mean and standard deviation of the neutron population and the sum of the precursor population for step reactivity

Method	Step size	$\alpha$	$E[n(t)]$	$\sigma[n(t)]$	$E\left[\sum_{i=1}^6 c_i(t)\right]$	$\sigma\left[\sum_{i=1}^6 c_i(t)\right]$
$\rho = 0.007, t = 0.001$						
MC		1.0	135.67	93.376	$4.464 \times 10^5$	7.8073
SPCA		1.0	134.55	91.242	$4.464 \times 10^5$	19.444
EM		1.0	139.57	92.042	$4.463 \times 10^5$	6.071
T1.5SO		1.0	139.57	92.047	$4.463 \times 10^5$	18.337
AEM	$h = 0.00001$	1.0	134.54	91.234	$4.464 \times 10^5$	19.235
ESM	$h = 0.00001$	1.0	134.96	6.8527	$4.464 \times 10^5$	2.529
DPKM	$h = 0.000025$	1.0	135.0		$4.464 \times 10^5$	
DMT	$h = 0.001$	0.98	140.122221	7.872980	446362.78	3.794234
DMT	$h = 0.001$	0.99	137.268228	7.746689	446361.57	3.657256
DMT	$h = 0.001$	1.0	134.613600	7.627336	446360.52	3.525117
DMT	$h = 0.001$	1.01	132.144579	7.514619	446359.63	3.397625
DMT	$h = 0.001$	1.02	129.848341	7.408245	446358.87	3.274607
DMT	$h = 0.0005$	0.98	141.287614	7.427251	446362.79	3.262914
DMT	$h = 0.0005$	0.99	138.120575	7.318368	446361.49	3.137738
DMT	$h = 0.0005$	1.0	135.195181	7.216352	446360.39	3.017724
DMT	$h = 0.0005$	1.01	132.493180	7.120848	446359.45	2.902478
DMT	$h = 0.0005$	1.02	129.997682	7.031509	446358.66	2.791808
DMT	$h = 0.0001$	0.98	142.454816	7.029539	446363.37	2.946374
DMT	$h = 0.0001$	0.99	138.562403	6.927727	446361.78	2.796684
DMT	$h = 0.0001$	1.0	135.024891	6.833936	446360.47	2.656922
DMT	$h = 0.0001$	1.01	131.810129	6.747624	446359.39	2.525245
DMT	$h = 0.0001$	1.02	128.888862	6.668273	446358.50	2.401280
$\rho = 0.003, t = 0.1$						
MC		1.0	183.04	168.79	$4.478 \times 10^5$	1495.7
SPCA		1.0	186.31	164.16	$4.491 \times 10^5$	1917.20
EM		1.0	208.60	255.95	$4.498 \times 10^5$	1233.38
T1.5SO		1.0	199.41	168.547	$4.497 \times 10^5$	1218.82
AEM	$h = 0.001$	1.0	186.30	164.14	$4.490 \times 10^5$	1911.91
ESM	$h = 0.001$	1.0	179.93	10.555	$4.489 \times 10^5$	94.75
DPKM	$h = 0.0025$	1.0	179.95		$4.489 \times 10^5$	
DMT	$h = 0.001$	0.98	180.922922	12.847182	449304.10	94.953085
DMT	$h = 0.001$	0.99	180.466893	13.190199	449083.17	94.453581
DMT	$h = 0.001$	1.0	180.036327	13.547699	448878.15	93.938513
DMT	$h = 0.001$	1.01	179.629458	13.919605	448687.88	93.403821
DMT	$h = 0.001$	1.02	179.244639	14.305915	448511.28	92.845214
DMT	$h = 0.0005$	0.98	181.064354	11.889735	449347.96	95.974066
DMT	$h = 0.0005$	0.99	180.562722	12.307332	449103.51	95.397178
DMT	$h = 0.0005$	1.0	180.093120	12.742279	448878.30	94.806707
DMT	$h = 0.0005$	1.01	179.653284	13.194207	448670.78	94.198372
DMT	$h = 0.0005$	1.02	179.241129	13.662739	448479.56	93.567468
DMT	$h = 0.0001$	0.98	180.596300	10.464344	449450.09	88.949000
DMT	$h = 0.0001$	0.99	179.988863	10.964650	449149.09	88.353100
DMT	$h = 0.0001$	1.0	179.435711	11.490519	448876.38	87.735258
DMT	$h = 0.0001$	1.01	178.932909	12.042888	448629.26	87.089442
DMT	$h = 0.0001$	1.02	178.476566	12.622634	448405.28	86.409072

different values of fractional order with the results of the traditional stochastic methods.

### 4.1 Step reactivity

The first computational example simulates two cases of step reactivity  $\rho = 0.007$  and  $\rho = 0.003$  for an actual reactor with six groups of delayed precursors [1]. The parameters of the two problems are taken from the following references [1, 5, 9, 11, 12] as follows:  $\nu = 2.5$ ,  $\Lambda = 0.00002$  s,  $n_0 = 100$  (neutrons),  $\lambda_i = [0.0127, 0.0317, 0.115, 0.311, 1.4, 3.87]$  s<sup>-1</sup>,  $\beta_i = [0.000266, 0.001491, 0.001316, 0.002849, 0.000896, 0.000182]$ ,  $\beta = 0.007$ , and  $q = 0$ . The mean and standard deviation at step size  $h = 0.001$  s after 500 trails are given in Table 1 for reactivity  $\rho = 0.007$  and time  $T = 0.001$  s. In the calculation of the

developed mathematical technique, the partial requests of the fractional order are taken, respectively, as:  $\alpha = 1$ ,  $\alpha = 0.98$ ,  $\alpha = 0.99$ ,  $\alpha = 1.01$ , and  $\alpha = 1.02$ . The Matlab code is tested with the conventional results under the same conditions. The obtained results of the developed mathematical technique (DMT) are compared with the familiar Monte Carlo (MC) [1], stochastic piecewise constant approximation (SPCA) [1], Euler–Maruyama (EM) [5], Taylor 1.5 strong order (T1.5SO) [5], analytical exponential model (AEM) [12], efficient stochastic model (ESM) [11], and the deterministic point kinetics model (DPKM) [33].

In a similar manner, the results of the second case  $\rho = 0.003$  are given in Table 1. The numerical results, in this case, are calculated at time  $t = 0.1$  s. Moreover, the pattern of the two individual neutron sample paths and the mean

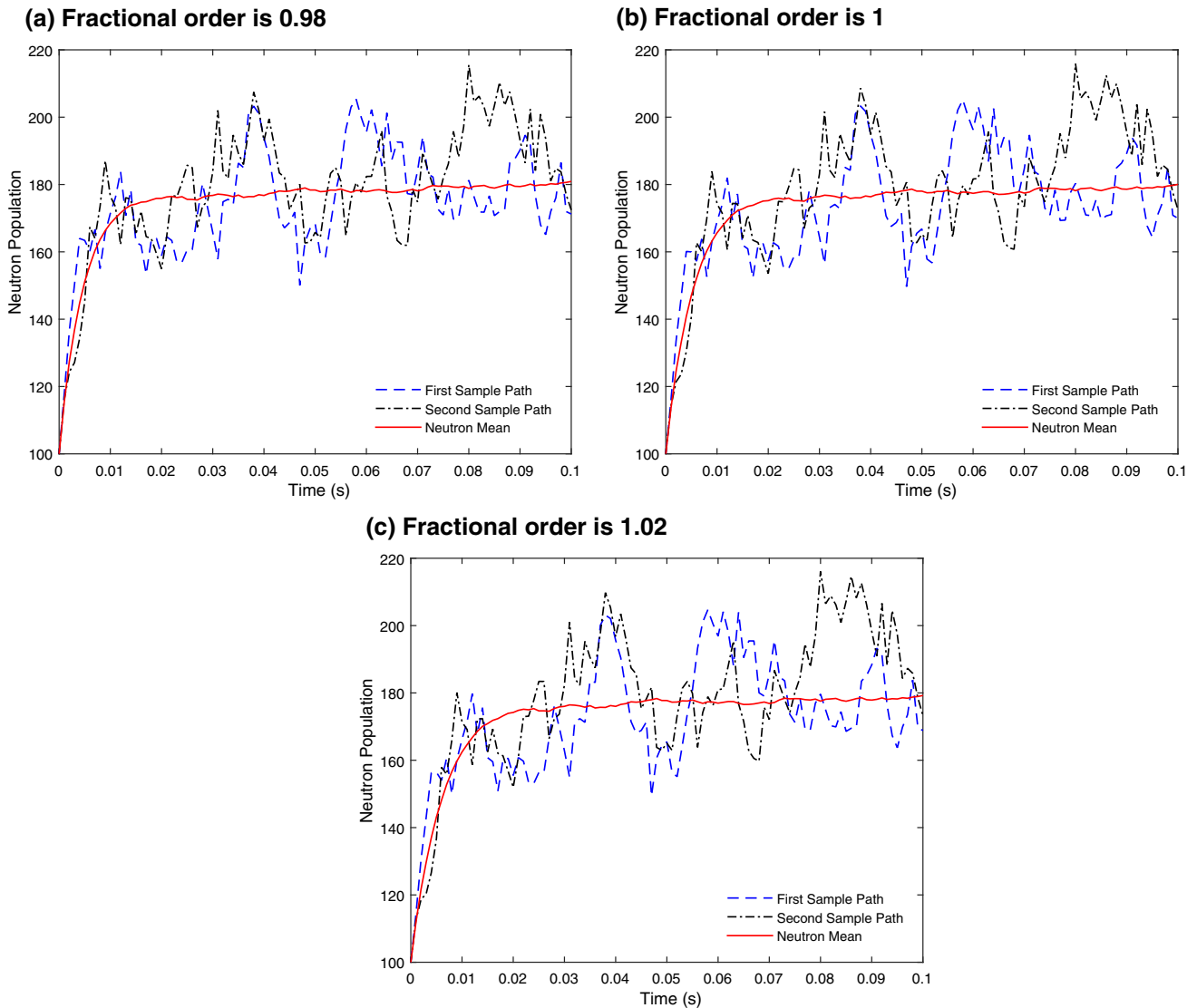


**Fig. 1** Mean neutron population and two individual neutron sample paths for various values of fractional order and step reactivity  $\rho = 0.003$

**Table 2** Mean and standard deviation of the neutron population and the sum of the precursor population for ramp reactivity  $\rho = 0.1\beta t$

Method	Step size	$\alpha$	$E[n(1)]$	$\sigma[n(1)]$	$E\left[\sum_{i=1}^6 c_i(1)\right]$	$\sigma\left[\sum_{i=1}^6 c_i(1)\right]$
SPCA	$h = 0.01$	1.0	113.268077	13.330142	448239.846	3009.93141
AEM	$h = 0.01$	1.0	113.267707	13.327291	448239.798	3002.68282
ESM	$h = 0.01$	1.0	113.116433	4.111150	448253.780	47.203115
DPKM	$h = 0.001$	1.0	113.091124		448236.26	
DMT	$h = 0.01$	0.98	113.474956	9.476546	448434.483	46.871815
DMT	$h = 0.01$	0.99	113.384203	9.473676	448331.161	46.840134
DMT	$h = 0.01$	1.0	113.296719	9.470503	448232.846	46.811703
DMT	$h = 0.01$	1.01	113.212358	9.468112	448139.299	46.782352
DMT	$h = 0.01$	1.02	113.131034	9.466234	448050.294	46.753327
DMT	$h = 0.001$	0.98	113.415094	3.971593	448535.015	43.751183
DMT	$h = 0.001$	0.99	113.280768	4.058934	448378.858	43.695078
DMT	$h = 0.001$	1.0	113.153337	4.150857	448233.774	43.632678
DMT	$h = 0.001$	1.01	113.032287	4.247468	448098.976	43.555908
DMT	$h = 0.001$	1.02	112.917106	4.348945	447973.736	43.348216
DMT	$h = 0.0001$	0.98	113.305430	3.263194	448638.295	47.552005
DMT	$h = 0.0001$	0.99	113.112671	3.411900	448425.709	47.488998
DMT	$h = 0.0001$	1.0	112.932052	3.567299	448232.798	47.438442
DMT	$h = 0.0001$	1.01	112.762814	3.729720	448057.756	47.366197
DMT	$h = 0.0001$	1.02	112.604169	3.899621	447898.902	47.283241

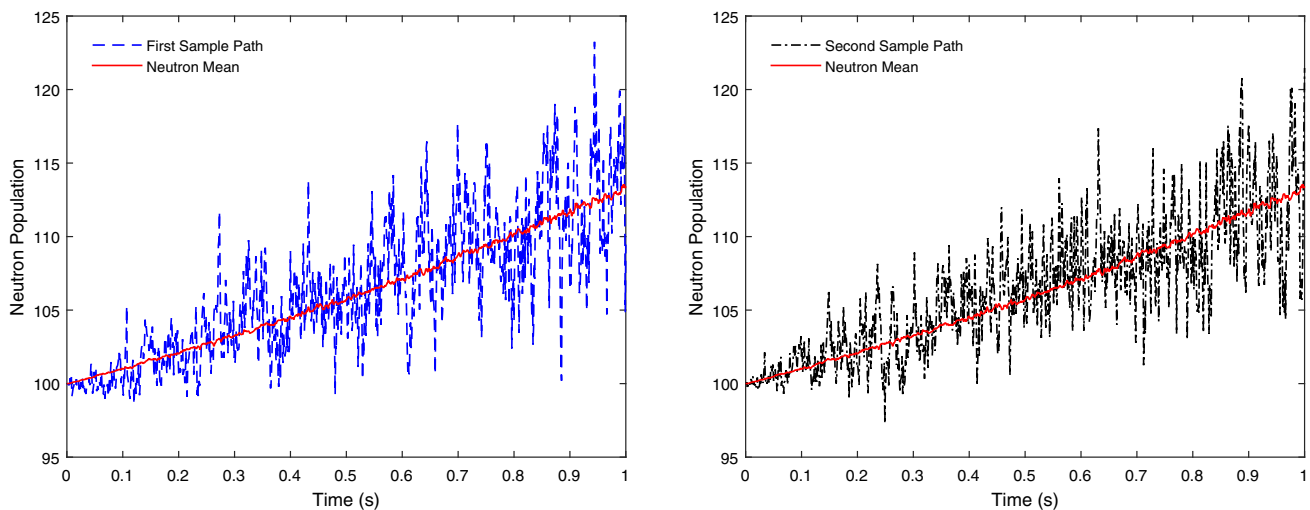


**Fig. 2** Mean neutron population and two individual neutron sample paths for fractional order 0.98 and ramp reactivity  $\rho = 0.1\beta t$

neutron population are shown in Fig. 1 at different values of the fractional order  $\alpha = 0.98$ ,  $\alpha = 1$ , and  $\alpha = 1.02$ , symbolized  $a$ ,  $b$ , and  $c$ , respectively. The red solid curve is the mean neutron population, while the blue dashed curve and black dot-dashed curve represent the two individual neutron sample paths, which show approximately a real behavior for neutron density into the actual reactors.

### 4.2 Ramp reactivity

The second example simulates a ramp reactivity, where the same parameters are taken from the previous example. The function of reactivity is taken as:  $\rho = 0.1\beta t$  and  $T = 1$  s. The result of a comparison of the proposed method (DMT), efficient stochastic model (ESM) [11], and the deterministic point kinetics model (DPKM) [33] is given in Table 2. To show the effect of the time interval, the code for the developed method was run at different time steps as well as at different values of the parameter  $\alpha$ . The

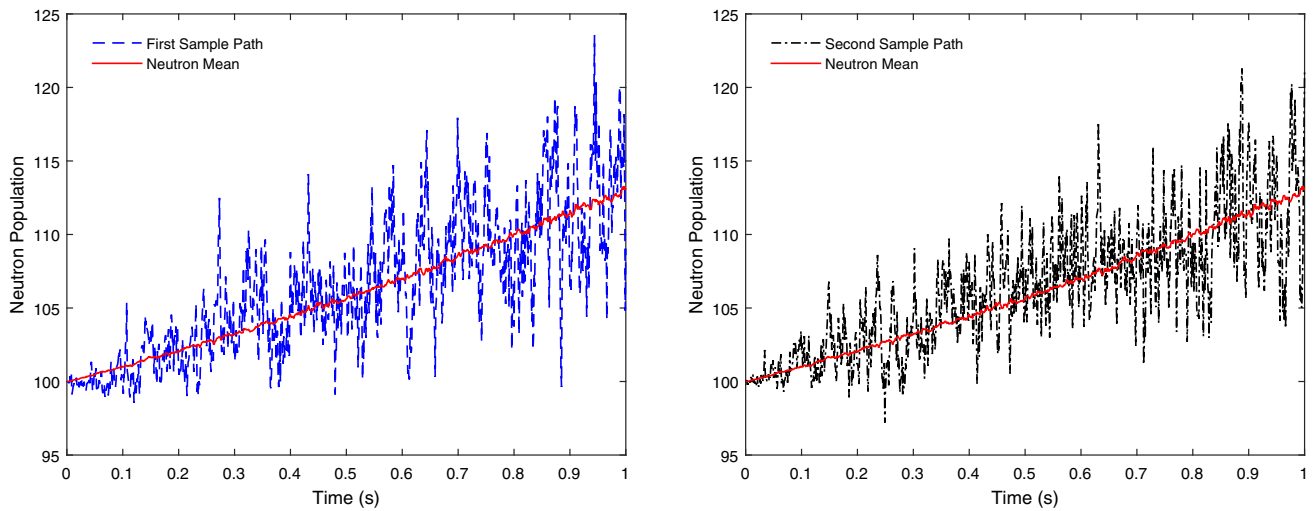


**Fig. 3** Mean neutron population and two individual neutron sample paths for fractional order 1.0 and ramp reactivity  $\rho = 0.1\beta t$

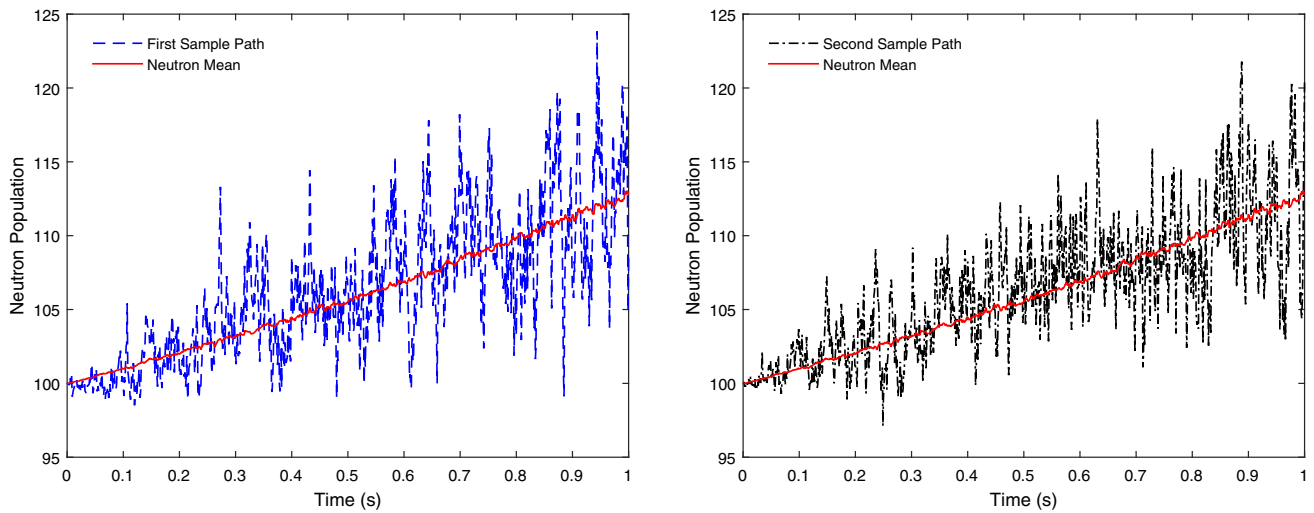


**Fig. 4** Mean neutron population and two individual neutron sample paths for fractional order 1.02 and ramp reactivity  $\rho = 0.1\beta t$

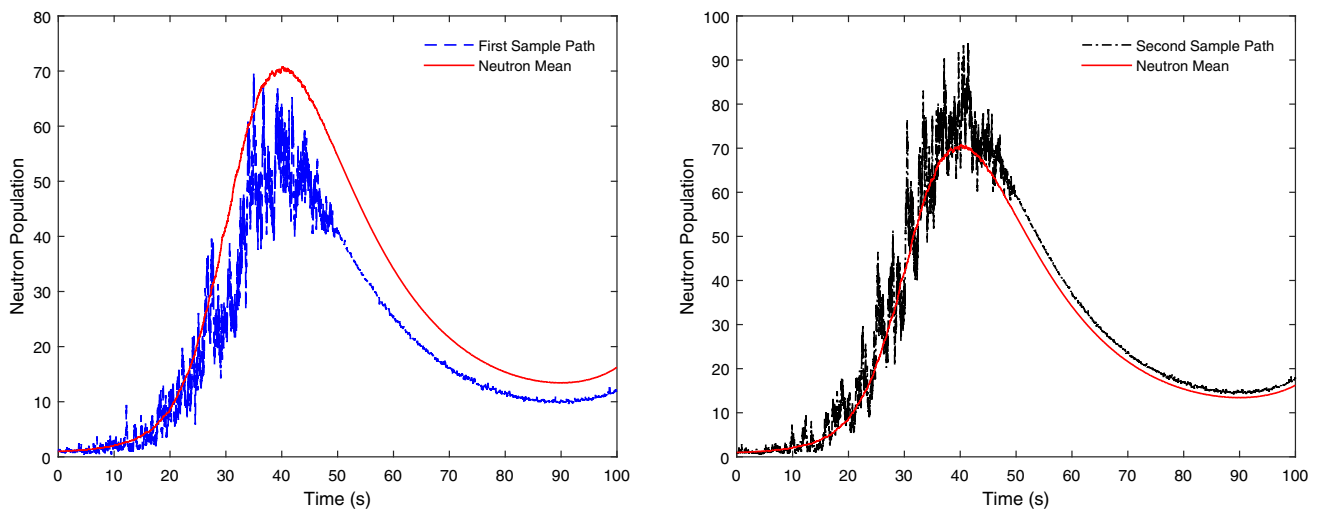


**Fig. 5** Mean neutron population and two individual neutron sample paths for fractional order 0.98 and sinusoidal reactivity  $\rho = 0.68\beta \sin(\frac{\pi t}{50})$

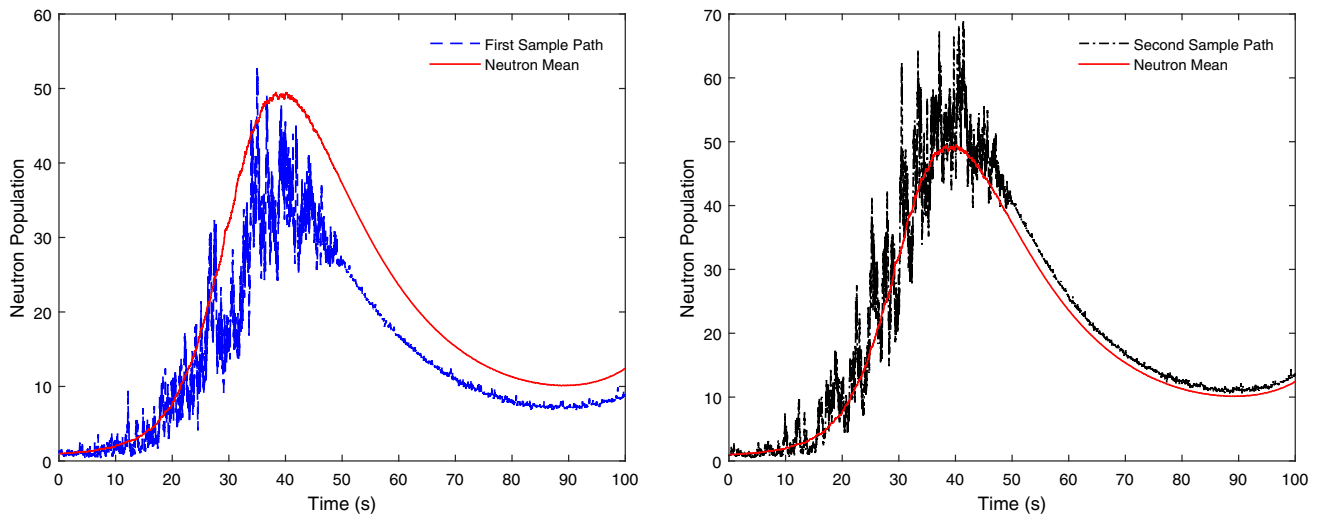


**Fig. 6** Mean neutron population and two individual neutron sample paths for fractional order 1.0 and sinusoidal reactivity  $\rho = 0.68\beta \sin(\frac{\pi t}{50})$

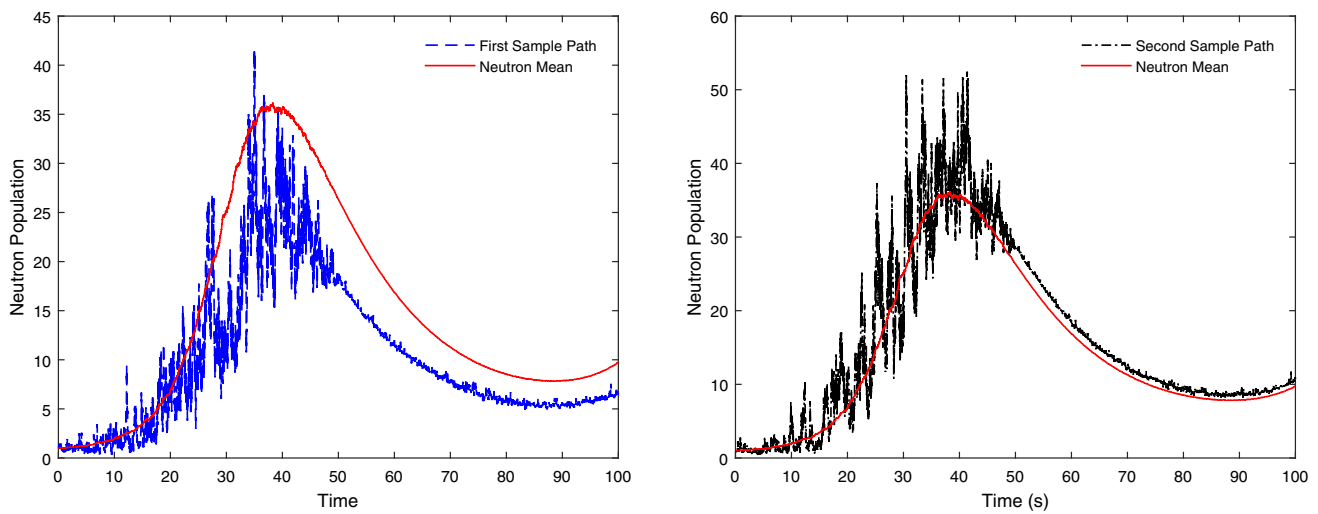


**Fig. 7** Mean neutron population and two individual neutron sample paths for fractional order 1.02 and sinusoidal reactivity  $\rho = 0.68\beta \sin(\frac{\pi t}{50})$

**Table 3** Peak of the mean neutron population and its time for the nonlinear fractional stochastic model at step external reactivity

Method	$\alpha$	$\rho_{ex}(\%)$	0.5	0.75	1.0	1.5	2.0
DMT	0.98	Peak	53.0279	189.727	895.547	41083.125	158278.694
		Time	25.378	7.732	0.942	0.151	0.088
	0.99	Peak	49.565	176.089	826.687	36557.357	140582.052
		Time	26.284	8.181	1.025	0.162	0.094
	1.0	Peak	46.289	163.986	768.739	34289.333	132756.323
		Time	28.142	8.762	1.09	0.173	0.101
1.01	Peak	43.137	152.776	712.311	30306.984	117251.348	
	Time	30.303	9.429	1.211	0.186	0.108	
1.02	Peak	40.239	142.525	662.795	28353.797	111465.515	
	Time	30.708	9.711	1.245	0.199	0.116	
AET	1.0	Peak	46.235334	164.209516	770.5188	33119.58	128083.1
		Time	28.142	8.867	1.040	0.174	0.101

relative percentage errors for  $E[n(t)]$  with the DMT are recorded as 0.025, 0.026, and 0.159 compared with the conventional methods SPCA, AEM, and ESM, respectively, under the same conditions at time step  $h = 0.01$  s, Table 2 for ramp reactivity, while the relative percentage error is 0.05 for the DPKM at time step  $h = 0.001$  s. Furthermore, in the same table, the relative percentage errors for the DMT method at different step time intervals ( $h = 0.01$  and  $h = 0.001$ ) are recorded as 0.126, while at  $h = 0.01$  and  $h = 0.0001$  it is 0.322. In Table 1 for step reactivity the effect of the time step interval appears from the relative percentage error at different time steps, e.g., at  $h = 0.001$  and  $h = 0.0005$  the RPE is  $-0.432$ , while at  $h = 0.001$  and  $h = 0.0001$  it is  $-0.306$ . The previous analysis confirms the stability of the DMT method, and the

effect of time step is acceptable. The behavior of the results shows an increase with the decreasing value of  $\alpha$  and vice versa. Finally, we conclude that the validity of the proposed method shows a high agreement with the deterministic method DPKM as well as with the conventional methods (e.g., MC, SPCA, EM, T1.5SO, AEM, ESM, and DMT).

For various values of fractional orders ( $\alpha = 0.98, \alpha = 1, \alpha = 1.02$ ), the pattern of the two individual neutron sample paths and the mean neutron are shown in Figs. 2, 3, and 4. Furthermore, the intensity of fluctuations for neutron sample paths increases with the mean neutron population. This phenomenon arises from the fact that the variance matrix including stochastic part is dependent on the mean neutron population and precursors population.

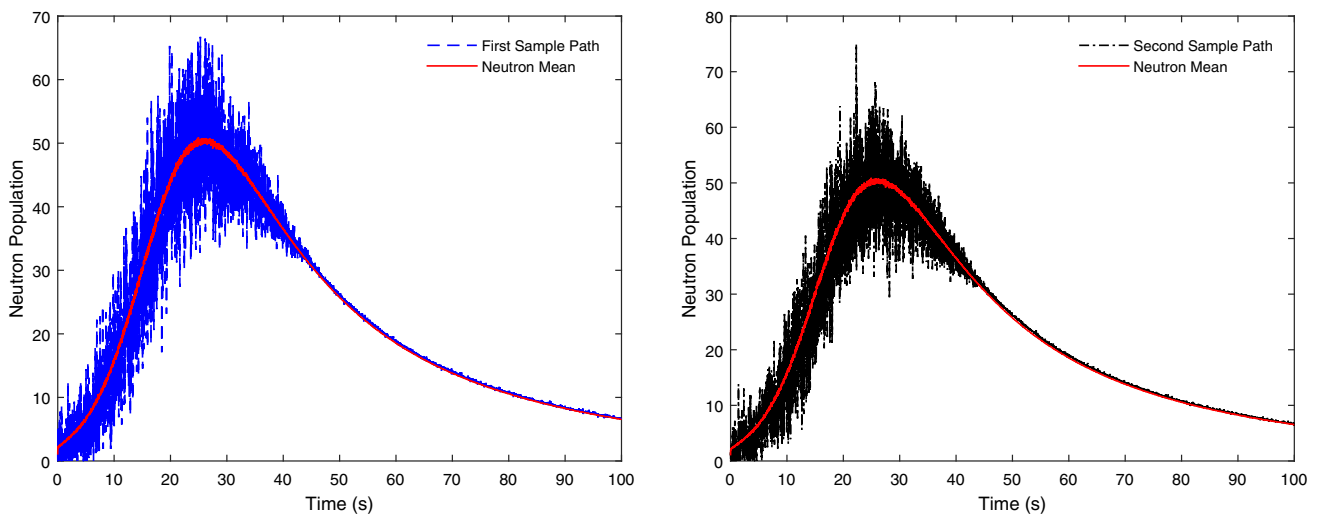


**Fig. 8** Mean neutron population and two individual neutron sample paths for fractional order 0.98 and temperature feedback reactivity  $\rho_{ex} = 0.5\%$  and  $\sigma = 2.5 \times 10^{-6}$

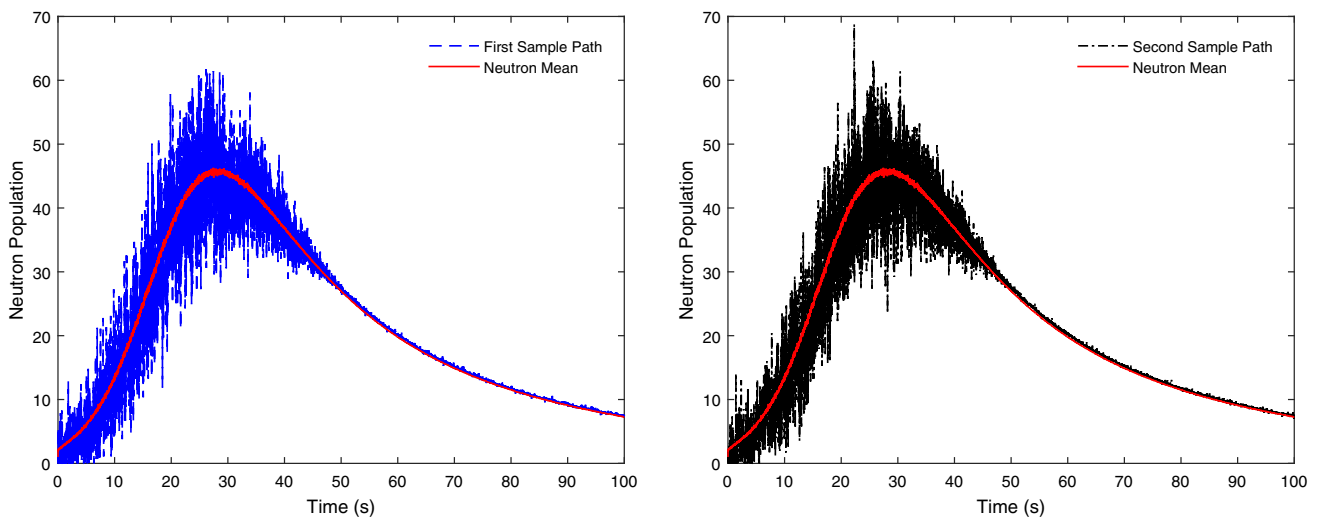


**Fig. 9** Mean neutron population and two individual neutron sample paths for fractional order 1.0 and temperature feedback reactivity  $\rho_{ex} = 0.5\%$  and  $\sigma = 2.5 \times 10^{-6}$

### 4.3 Sinusoidal reactivity

In the third example, the variation of reactivity insertion in the form of a sinusoidal change as  $\rho = \rho_0 \sin(\frac{\pi t}{T})$  [6] is considered. The parameters of the nuclear reactor with one group of delayed neutrons are as follows:  $\rho_0 = 0.005333(0.68\%)$ ,  $\beta_1 = \beta = 0.0079$ ,  $\lambda_1 = 0.077$ ,  $\Lambda = 10^{-3}$ ,  $q = 0$ , and  $n_0 = 1$ (neutrons) with period time of  $2T = 100$  s. The two individual neutron sample paths and the mean neutron are shown in Figs. 5, 6, and 7 using different values of fractional orders ( $\alpha = 0.98$ ,  $\alpha = 1$ ,  $\alpha = 1.02$ ), respectively, where the time step interval is  $h = 0.01$  s after 500 trails. We compared the stochastic and deterministic solutions to deduce the fact that the

deterministic solution represents the average of the stochastic approach. Moreover, the individual sample paths oscillate around the deterministic curve. The intensity of fluctuations in these classes of figures arises from the variations of the mean neutron population.

### 4.4 Temperature feedback reactivity

In the most nuclear literature, there are two cases for the external reactivity, step, and ramp external reactivities. The means of the neutron population are calculated for a  $U^{235}$  nuclear reactor with step and ramp external reactivities. In what follows, the effect of Newtonian temperature feedback introduced into the reactivity is analyzed. The new

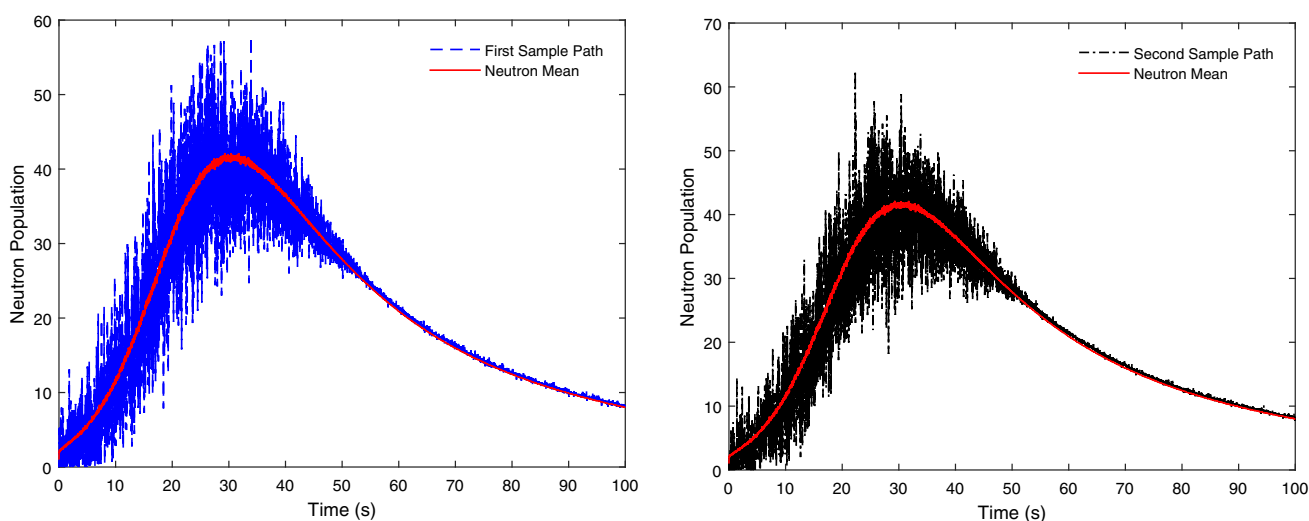


**Fig. 10** Mean neutron population and two individual neutron sample paths for fractional order 1.02 and temperature feedback reactivity  $\rho_{ex} = 0.5\%$  and  $\sigma = 2.5 \times 10^{-6}$

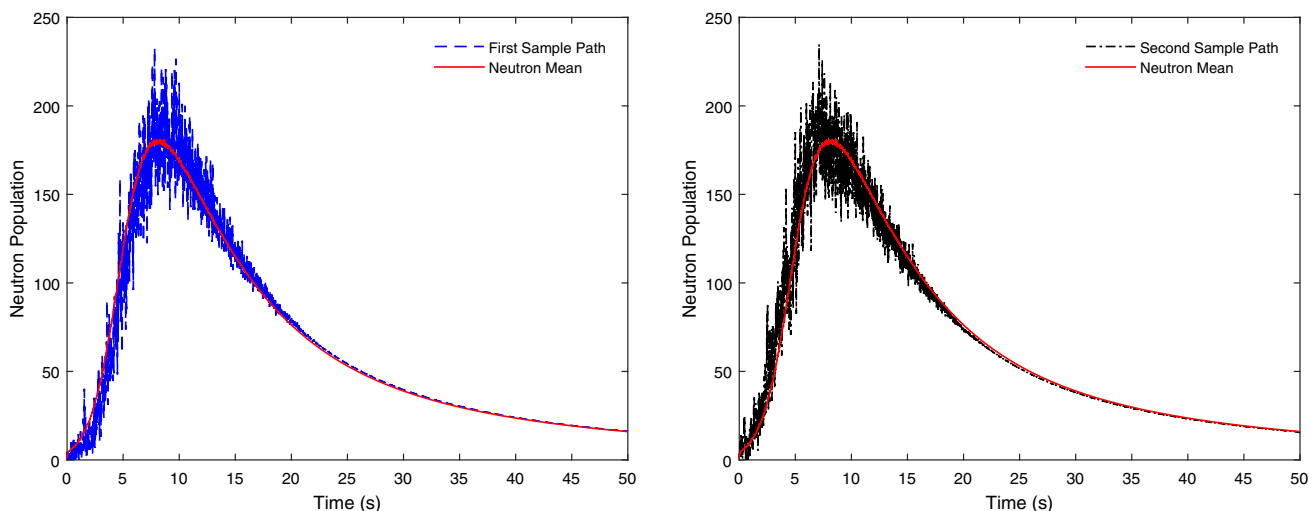


**Fig. 11** Mean neutron population and two individual neutron sample paths for fractional order 0.98 and temperature feedback reactivity  $\rho_{ex} = 0.75\%$  and  $\sigma = 2.5 \times 10^{-6}$

reactivity form in the presence of temperature feedback is given by:

$$\rho(t) = \rho_{\text{ex}}(t) - \sigma \int_0^t N(\tau) d\tau, \tag{24}$$

where  $\rho_{\text{ex}}(t)$  represents the external reactivity and  $\sigma$  is the nonlinear coefficient part which represents the product of the reciprocal of the thermal capacity and the temperature coefficient.

#### 4.4.1 Step external reactivity

To check the developed mathematical technique for the nonlinear fractional stochastic model in the presence of temperature feedback and step external reactivity, let us

take the parameters of the  $U^{235}$  nuclear reactor as follows [14, 15, 34]:  $\lambda_i = [0.0124, 0.0305, 0.111, 0.301, 1.13, 3.0] \text{ s}^{-1}$ ,  $\beta_i = [0.00021, 0.00141, 0.00127, 0.00255, 0.00074, 0.00027, 0.00645]$ ,  $\beta = 0.00645$ ,  $\Lambda = 5.0 \times 10^{-5} \text{ s}$ ,  $\sigma = 2.5 \times 10^{-6} \text{ (MWs)}^{-1}$ , and  $N(0) = 1 \text{ (neutrons)}$ .

In Table 3, the peak of the mean neutron population with the corresponding time at various step external reactivities,  $\rho_{\text{ex}} = 1.0\%$ ,  $\rho_{\text{ex}} = 1.5\%$ , and  $\rho_{\text{ex}} = 2\%$ , is given for different values of fractional order 0.98, 0.99, 1.0, 1.01, and 1.02. Using time step  $h = 0.001 \text{ s}$  and after 500 trails, the peak of the mean neutron population is compared with the peak of the mean neutron population using the analytical exponential technique (AET) [14]. In addition, the mean neutron population and the two individual neutron sample

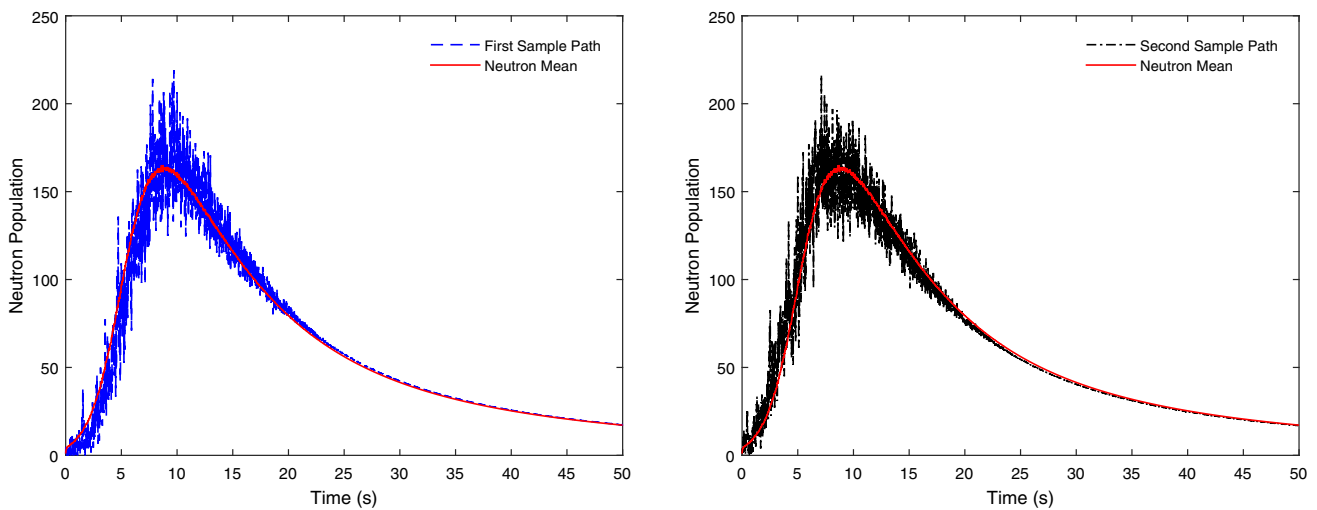


**Fig. 12** Mean neutron population and two individual neutron sample paths for fractional order 1.0 and temperature feedback reactivity  $\rho_{\text{ex}} = 0.75\%$  and  $\sigma = 2.5 \times 10^{-6}$

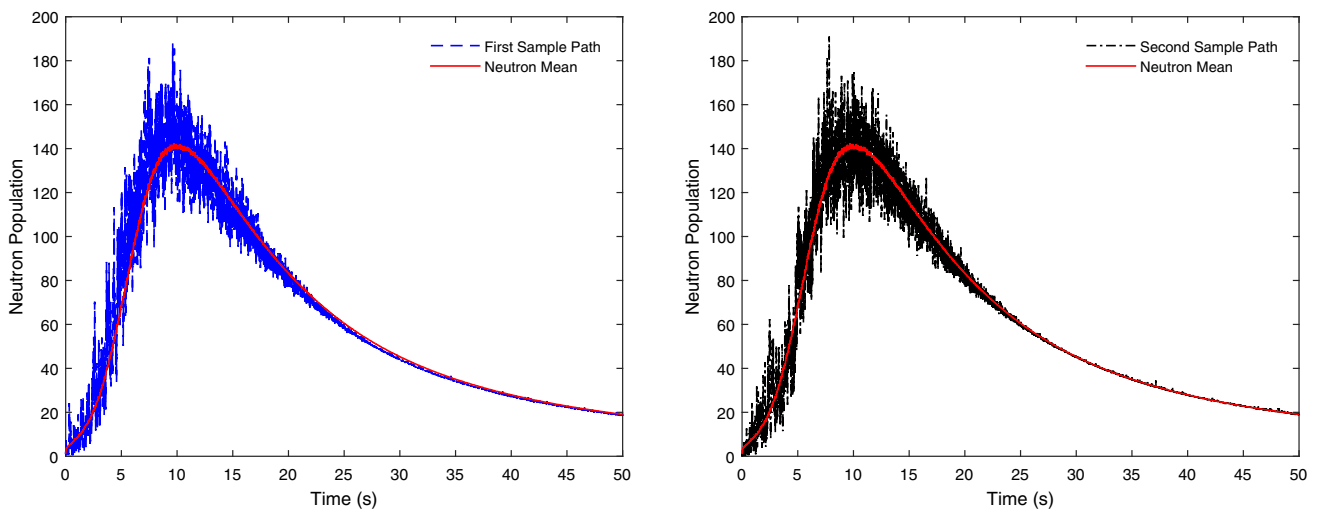


**Fig. 13** Mean neutron population and two individual neutron sample paths for fractional order 1.02 and temperature feedback reactivity  $\rho_{\text{ex}} = 0.75\%$  and  $\sigma = 2.5 \times 10^{-6}$

paths are plotted in Figs. 8, 9, and 10 for the step external reactivity ( $\rho_{ex} = 0.5\%$ ) and Figs. 11, 12, and 13 for the step external reactivity ( $\rho_{ex} = 0.75\%$ ) using different values of fractional derivative order 0.98, 1.0, and 1.02, respectively. The most important notice is that the mean neutron population increases with time until it reaches the maximum value due to the positive external reactivity. Thereafter, the

mean neutron tends to zero with the increasing time due to the effect of temperature reactivity feedback. Again, these figures confirm that the amplitude of fluctuations for neutron sample paths is affected by the direct variations of the mean neutron population.

**Table 4** Peak of the mean neutron population and its time for the nonlinear fractional stochastic model at reactivity  $\rho(t) = at - \sigma \int_0^t N(\tau)d\tau$

$\alpha$		$a = 0.003$		$a = 0.01$		$a = 0.1$	
		$\sigma = 10^{-11}$	$\sigma = 10^{-13}$	$\sigma = 10^{-11}$	$\sigma = 10^{-13}$	$\sigma = 10^{-11}$	$\sigma = 10^{-13}$
<b>DMT</b>							
0.98	Peak	$4.409101 \times 10^9$	$5.771654 \times 10^{11}$	$1.701579 \times 10^{10}$	$2.144910 \times 10^{12}$	$1.876758 \times 10^{11}$	$2.242436 \times 10^{13}$
	Time	2.446	2.488	0.831	0.852	0.130	0.136
0.99	Peak	$4.452107 \times 10^9$	$5.813629 \times 10^{11}$	$1.704601 \times 10^{10}$	$2.124988 \times 10^{12}$	$1.918749 \times 10^{11}$	$2.290324 \times 10^{13}$
	Time	2.461	2.504	0.839	0.861	0.132	0.138
1.0	Peak	$4.477012 \times 10^9$	$5.828427 \times 10^{11}$	$1.689973 \times 10^{10}$	$2.102489 \times 10^{12}$	$1.849657 \times 10^{11}$	$2.146883 \times 10^{13}$
	Time	2.475	2.520	0.847	0.869	0.135	0.142
1.01	Peak	$4.505250 \times 10^9$	$5.847340 \times 10^{11}$	$1.673285 \times 10^{10}$	$2.081893 \times 10^{12}$	$1.860123 \times 10^{11}$	$2.233038 \times 10^{13}$
	Time	2.491	2.537	0.856	0.879	0.138	0.144
1.02	Peak	$4.514868 \times 10^9$	$5.844036 \times 10^{11}$	$1.656222 \times 10^{10}$	$2.059339 \times 10^{12}$	$1.786014 \times 10^{11}$	$2.131587 \times 10^{13}$
	Time	2.507	2.554	0.864	0.888	0.141	0.148
<b>AET</b>							
1.0	Peak	$4.482853 \times 10^9$	$5.833649 \times 10^{11}$	$1.687565 \times 10^{10}$	$2.099857 \times 10^{12}$	$1.853996 \times 10^{11}$	$2.217193 \times 10^{13}$
	Time	2.476	2.521	0.847	0.870	0.135	0.141

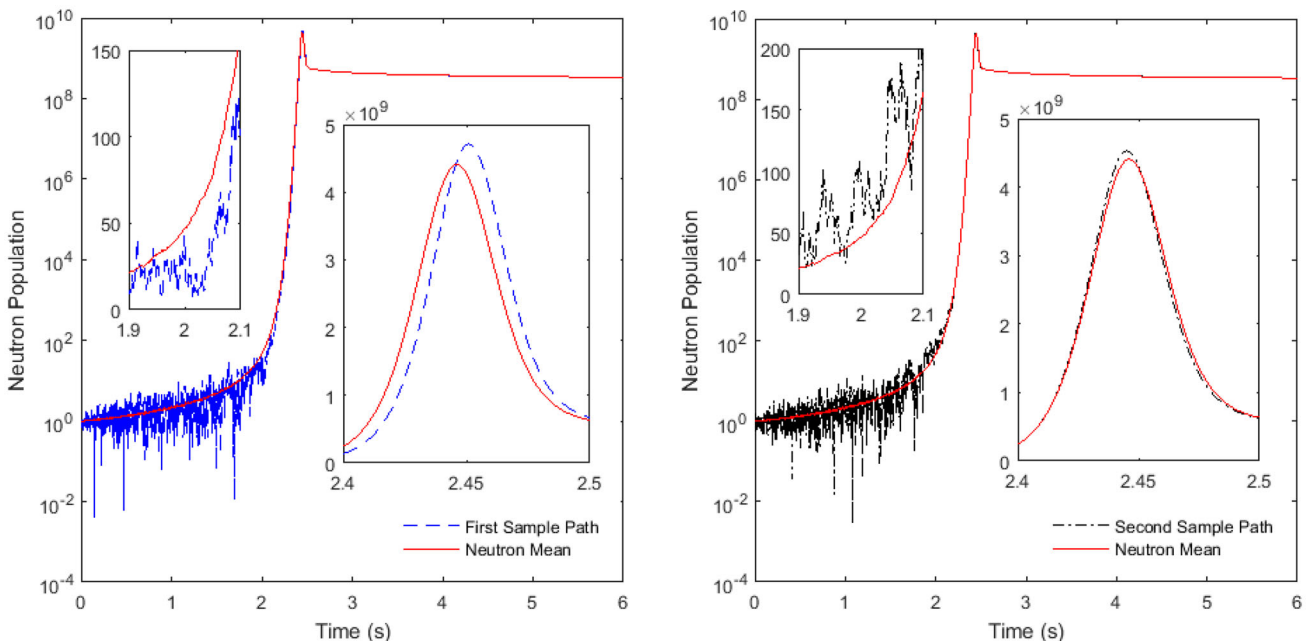


**Fig. 14** Mean neutron population and two individual neutron sample paths for fractional order 0.98, temperature feedback reactivity  $\rho_{ex} = 0.003t$  and  $\sigma = 10^{-11}$

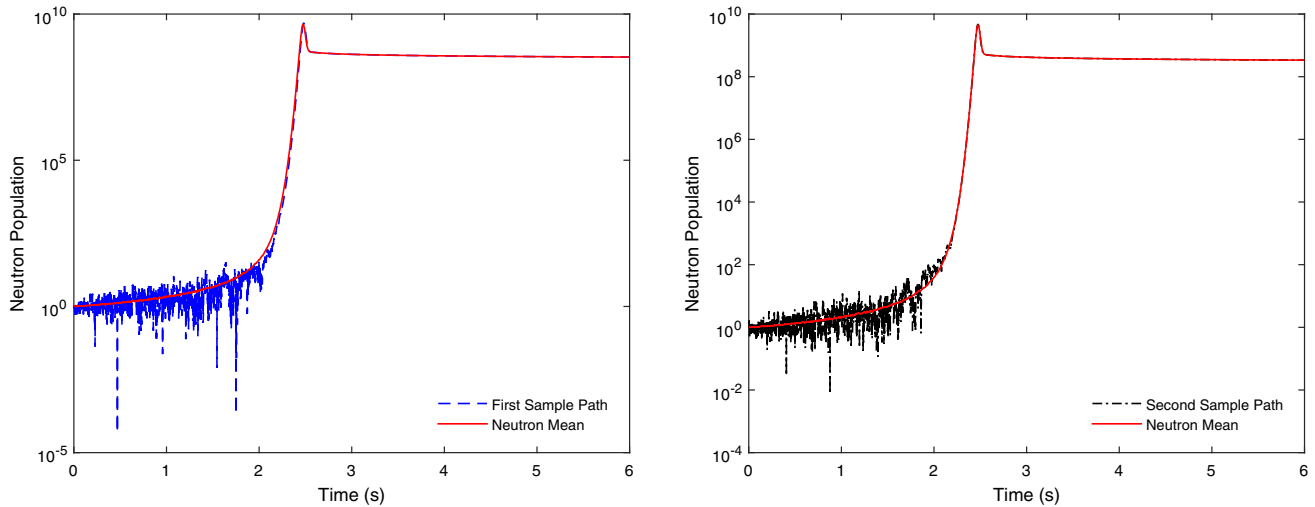


**Fig. 15** Mean neutron population and two individual neutron sample paths for fractional order 1.0, temperature feedback reactivity  $\rho_{ex} = 0.003t$  and  $\sigma = 10^{-11}$

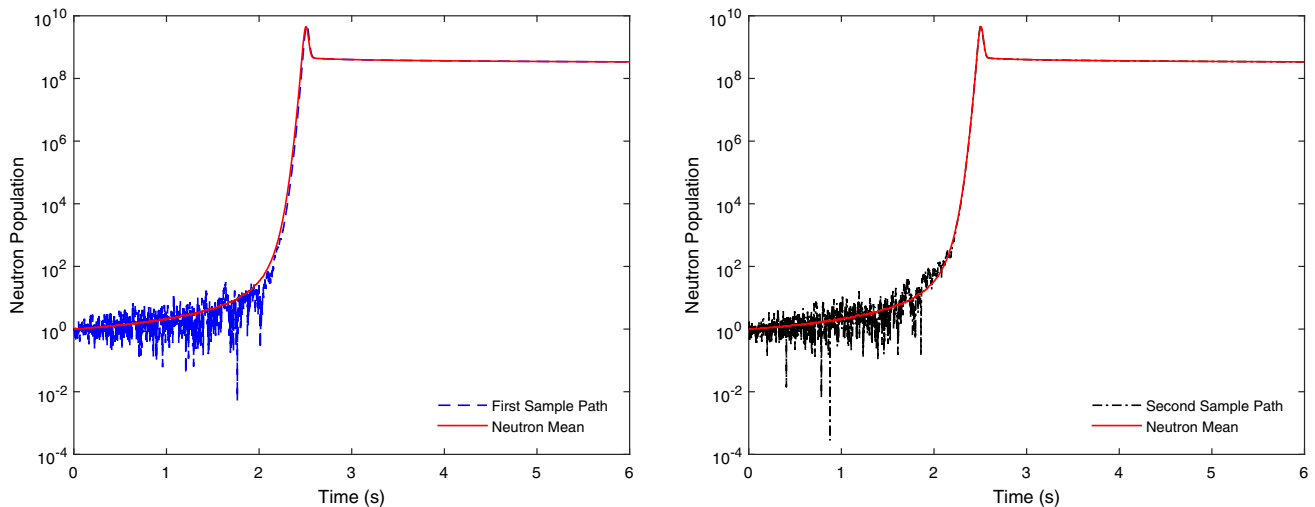


**Fig. 16** Mean neutron population and two individual neutron sample paths for fractional order 1.02, temperature feedback reactivity  $\rho_{ex} = 0.003t$  and  $\sigma = 10^{-11}$

4.4.2 Ramp external reactivity

In the test example for ramp external reactivity, the parameters for the  $U^{235}$  nuclear reactor are taken as the same values from the nonlinear case, where  $\Lambda = 10 \times 10^{-5} \text{ s}$ ,  $\sigma = 10^{-11}$ , or  $10^{-13} \text{ (MW s)}^{-1}$  and the external reactivity is ramp ( $\rho_{ex} = 0.01t, 0.1t$ ). The peak of the mean neutron population and its time with various values of fractional order (0.98, 1.0, 1.02) are compared with the results of the analytical exponential technique (AET) [14] in Table 4. The results are calculated with time step  $h = 0.001 \text{ s}$ , and the number of trails is 500. In addition, two individual neutron sample paths and the mean neutron population are drawn for external reactivity  $\rho_{ex}(t) = 0.003t$  and the nonlinear coefficient  $\sigma = 10^{-11}$  in

Figs. 14, 15, and 16 and  $\sigma = 10^{-13}$  in Figs. 17, 18, and 19. In Figs. 14, 15, 16, 17, 18, and 19, the mean neutron increases with time until it reaches the peak due to the external reactivity increasing. After that, the mean neutron decreases due to the effect of temperature feedback. Therefore, the mean neutron population is almost stable due to the effect of external reactivity, which is equivalent with the effect of temperature feedback. Moreover, the fluctuations of neutron sample paths disappear approximately around the sharp peak due to the logarithmic scale and a large increase in the neutron population at a very small time. Figure 14 shows a pattern of the effect of the neutron population and fluctuations at different sections with time. A sharp increase in fluctuation with a slight increase in the neutron population in the ramp section is

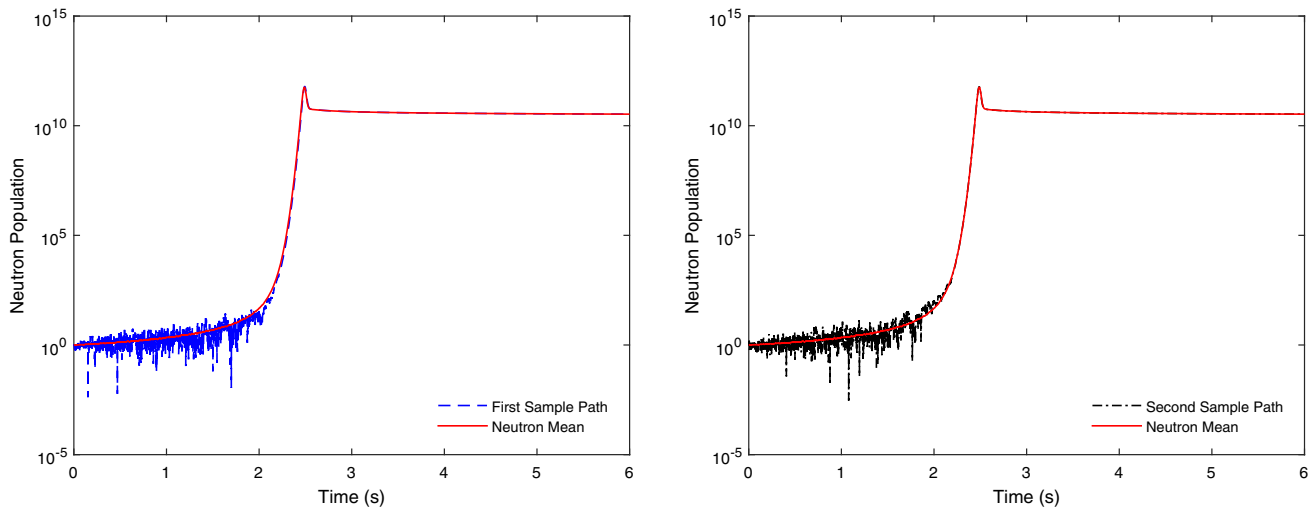


**Fig. 17** Mean neutron population and two individual neutron sample paths for fractional order 0.98, temperature feedback reactivity  $\rho_{ex} = 0.003t$  and  $\sigma = 10^{-13}$

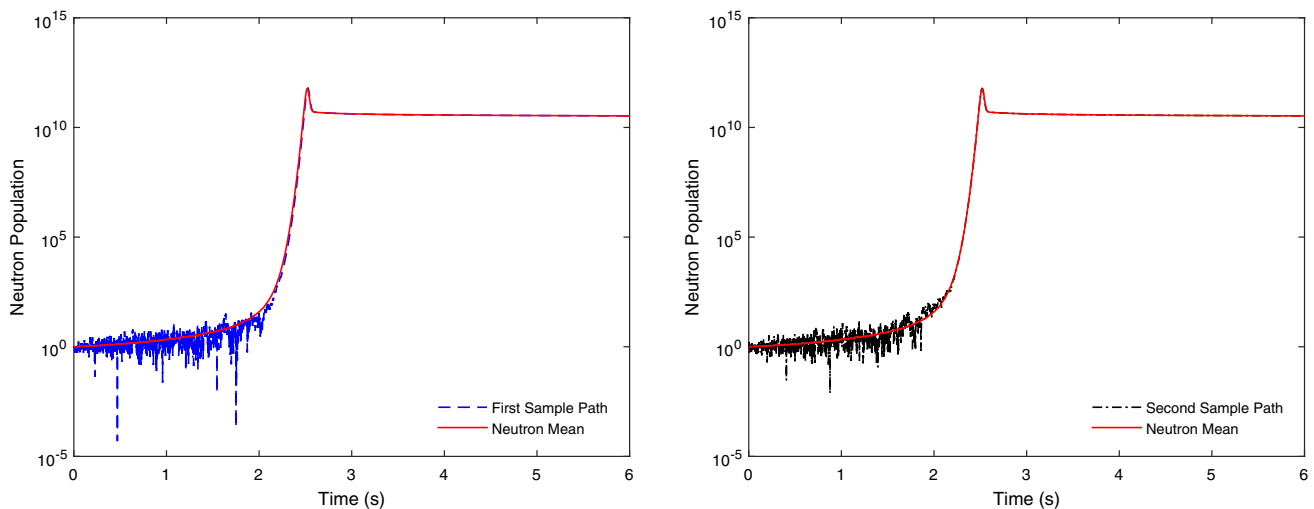


**Fig. 18** Mean neutron population and two individual neutron sample paths for fractional order 1.0, temperature feedback reactivity  $\rho_{ex} = 0.003t$  and  $\sigma = 10^{-13}$

followed by a slight increase in the intensity of fluctuations compared with a sharp increase in the neutron population. Moreover, the same remark is observed at the peak and the remainder section of the figures.

General description and analysis for the results of the developed method can be summarized as follows. Figures 1, 2, 3, 4, 5, 6, and 7 show a large class of changes consists of small variations of the cross sections, positive or negative changes in reactivity attributed to the neutron population, around an expected value  $E[n(t)]$ , corresponding to a critical case in which the perturbation can be induced flux fluctuations, where:  $\delta n(t) = n(t) - E[n(t)]$  and  $\delta \rho(t) = \rho(t) - E[\rho(t)]$ .

High-frequency power fluctuations caused by increasing the reactivity (the fission rate is sufficiently large for the

average value equations) of the reactor, as shown in Figs. 1, 2, 3, and 4. In the opposite, low-frequency power fluctuations can arise from decreasing the reactivity (i.e., the fission rate) as shown in Figs. 5, 6, 7, 8, 9, 10, 11, 12, and 13. Furthermore, Figs. 14, 15, 16, 17, 18, and 19 deal with the variation of the neutron population, which obtained by studying the fluctuations arise from the temperature feedback. These figures conclude that the randomness of the input is communicated to the output via the response characteristics of the system, where the fluctuation is above or below the mean value at instant time.

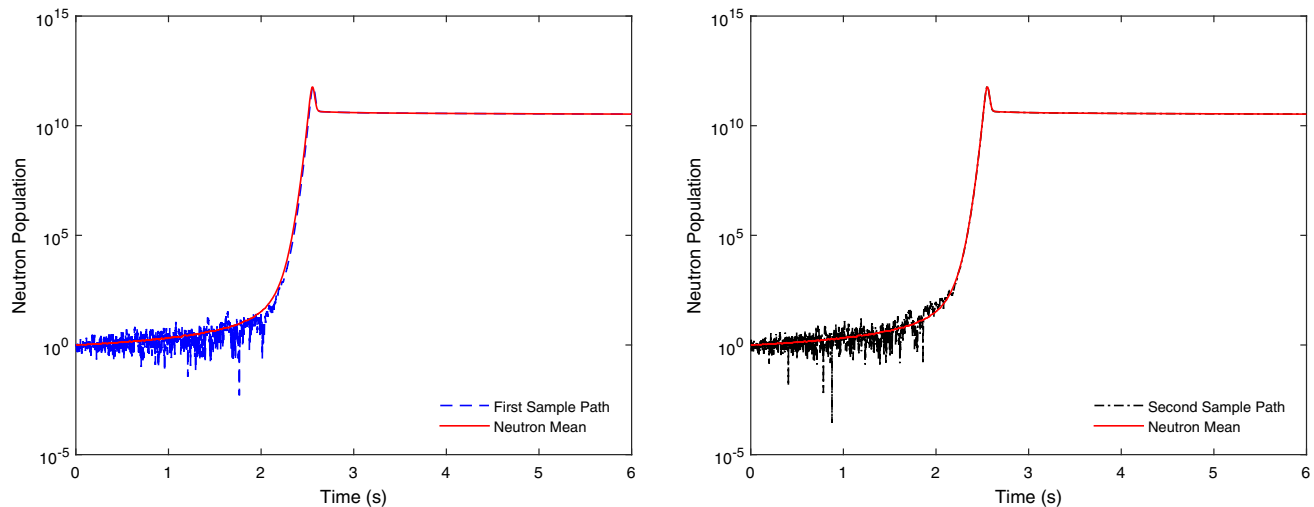


**Fig. 19** Mean neutron population and two individual neutron sample paths for fractional order 1.02, temperature feedback reactivity  $\rho_{ex} = 0.003t$  and  $\sigma = 10^{-13}$

## 5 Conclusion

The developed mathematical technique was presented for a linear/nonlinear fractional stochastic model of the point reactor kinetics system with a multi-group of delayed neutron precursors. This system is characterized by its stochastic behavior and can offer the only average or mean values of the modeled populations. However, the neutron population and the delayed neutron precursor concentrations vary randomly with time, meaning the real dynamical process is stochastic. This system was numerically implemented using a stochastic piecewise constant approximation (SPCA) due to the stiffness of these equations. In this paper, the matrix formula for this fractional stochastic model is solved through a developed mathematical technique, which is based on the split-step method, Laplace transforms, Mittag-Leffler function, eigenvalues, and eigenvectors. The mean and standard deviation of the neutron population and the sum of the precursor population were calculated for step, ramp, sinusoidal, and the temperature feedback reactivity insertion which represents the nonlinear fractional stochastic model. Moreover, this fractional differential system was calculated with different values of the fractional derivative order. In order to validate the proposed method (DMT), we present a comparison with the conventional results in the literature of the stochastic model and the deterministic point kinetics model, showing that the method is in agreement with those already established. The future work will be included the derivation and the study of a fractional stochastic model for the time-space kinetics equations.

## References

1. J.G. Hayes, E.J. Allen, Stochastic point kinetics equations in nuclear reactor dynamics. *Ann. Nucl. Energy* **32**, 572–587 (2005). <https://doi.org/10.1016/j.anucene.2004.11.009>
2. J.G. Hayes, Development of stochastic point kinetics equations in nuclear reactor dynamics, thesis, Texas Tech University (2005). <https://ttu-ir.tdl.org/ttu-ir/bitstream/handle/2346/22276/HayesThesis.pdf>
3. P.N. Ha, J.K. Kim, A stochastic approach to monoenergetic space-time nuclear reactor kinetics. *J. Nucl. Sci. Technol.* **47**, 705–711 (2010). <https://doi.org/10.1080/18811248.2010.9711646>
4. P.N. Ha, J.K. Kim, Further evaluation of a stochastic model applied to monoenergetic space-time nuclear reactor kinetics. *Nucl. Eng. Technol.* **43**, 523–530 (2011). <https://doi.org/10.5516/NET.2011.43.6.523>
5. S.S. Ray, Numerical simulation of stochastic point kinetic equation in the dynamical system of nuclear reactor. *Ann. Nucl. Energy* **49**, 154–159 (2012). <https://doi.org/10.1016/j.anucene.2012.05.022>
6. S.S. Ray, A. Patra, Numerical solution for stochastic point kinetics equations with sinusoidal reactivity in dynamical system of nuclear reactor. *Int. J. Nucl. Energy Sci. Technol.* **7**, 231–242 (2013). <https://doi.org/10.1504/IJNEST.2013.052165>
7. E.J. Allen, Stochastic difference equations and a stochastic partial differential equation for neutron transport. *J. Differ. Equ. Appl.* **18**, 1267–1285 (2012). <https://doi.org/10.1080/10236198.2010.488229>
8. E.J. Allen, A stochastic analysis of power doubling time for a subcritical system. *Stoch. Anal. Appl.* **31**, 528–537 (2013). <https://doi.org/10.1080/07362994.2013.777287>
9. S.S. Ray, A. Patra, Numerical solution of fractional stochastic neutron point kinetic equation for nuclear reactor dynamics. *Ann. Nucl. Energy* **54**, 154–161 (2013). <https://doi.org/10.1016/j.anucene.2012.11.007>
10. S.M. Ayyoubzadeh, N. Vosoughi, An alternative stochastic formulation for the point kinetics. *Ann. Nucl. Energy* **63**, 691–695 (2014). <https://doi.org/10.1016/j.anucene.2013.09.013>
11. A.A. Nahla, A.M. Edress, Analytical exponential model for stochastic point kinetics equations via eigenvalues and eigenvectors. *Nucl. Sci. Technol.* **27**(20), 1–8 (2016). <https://doi.org/10.1007/s41365-016-0025-6>

12. A.A. Nahla, A.M. Edress, Efficient stochastic model for the point kinetics equations. *Stoch. Anal. Appl.* **34**, 598–609 (2016). <https://doi.org/10.1080/07362994.2016.1159519>
13. M.W. da Silva, R. Vasques, B.E.G. Bodmann et al., A nonstiff solution for the stochastic neutron point kinetics equations. *Ann. Nucl. Energy* **97**, 47–52 (2016). <https://doi.org/10.1016/j.anucene.2016.06.026>
14. A.A. Nahla, Stochastic model for the nonlinear point reactor kinetics equations in the presence Newtonian temperature feedback effects. *J. Differ. Equ. Appl.* **23**, 1003–1016 (2017). <https://doi.org/10.1080/10236198.2017.1308507>
15. S. Singh, S.S. Ray, On the comparison of two split-step methods for the numerical simulation of stochastic point kinetics equations in presence of Newtonian temperature feedback effects. *Ann. Nucl. Energy* **110**, 865–873 (2017). <https://doi.org/10.1016/j.anucene.2017.08.001>
16. E.J. Allen, *Modeling with Itô Stochastic Differential Equations* (Springer, Dordrecht, 2007)
17. D.J. Higham, An algorithmic introduction to numerical simulation of stochastic differential equations. *SIAM Rev.* **43**, 525–546 (2001). <https://doi.org/10.1137/S0036144500378302>
18. M.A. Akinlar, A. Secer, M. Bayram, Numerical solution of fractional Benney equation. *Appl. Math.* **8**, 1633–1637 (2014). <https://doi.org/10.12785/amis/080418>
19. M. Caputo, *Elasticità Dissipazione* (Zanichelli, Bologna, 1969)
20. I. Podlubny, *Fractional Differential Equations* (Academic Press, San Diego, 1999)
21. S.S. Ray, *Fractional Calculus with Applications for Nuclear Reactor Dynamics* (CRC Press, Taylor and Francis group, Boca Raton, New York, 2016)
22. M.M.R. Williams, *Random Processes in Nuclear Reactors* (Pergamon Press, Oxford, 1974)
23. S. Kazem, Exact solution of some linear fractional differential equations by Laplace transform. *Int. J. Nonlin. Sci.* **16**, 3–11 (2013)
24. A.A. Nahla, Analytical solution of the fractional point kinetics equations with multigroup of delayed neutrons during start-up of a nuclear reactor. *Ann. Nucl. Energy* **99**, 247–252 (2017). <https://doi.org/10.1016/j.anucene.2016.08.030>
25. A.A. Nahla, A. Hemeda, Picard iteration and Padé approximations for stiff fractional point kinetics equations. *Appl. Math. Comput.* **293**, 72–80 (2017). <https://doi.org/10.1016/j.amc.2016.08.008>
26. A.E. Aboanber, Stiffness treatment of differential equations for the point reactor dynamic systems. *Prog. Nucl. Energy* **71**, 248–257 (2014). <https://doi.org/10.1016/j.pnucene.2013.12.004>
27. A.A. Nahla, Analytical solution to solve the point reactor kinetics equations. *Nucl. Eng. Des.* **240**, 1622–1629 (2010). <https://doi.org/10.1016/j.nucengdes.2010.03.003>
28. J.A.M. Nobrega, A new solution of the point kinetics equations. *Nucl. Sci. Eng.* **46**, 366–375 (1971)
29. A.E. Aboanber, A.A. Nahla, Generalization of the analytical inversion method for the solution of the point kinetics equations. *J. Phys. A Math. Gen.* **35**, 3245–3263 (2002). <https://doi.org/10.1088/0305-4470/35/14/307>
30. A.E. Aboanber, A.A. Nahla, Solution of the point kinetics equations in the presence of Newtonian temperature feedback by Padé approximations via the analytical inversion method. *J. Phys. A Math. Gen.* **35**, 9609–9627 (2002). <https://doi.org/10.1088/0305-4470/35/45/309>
31. A.A. Nahla, Generalization of the analytical exponential model to solve the point kinetics equations of Be- and  $D_2O$ -moderated reactors. *Nucl. Eng. Des.* **238**, 2648–2653 (2008). <https://doi.org/10.1016/j.nucengdes.2008.04.002>
32. A.A. Nahla, An efficient technique for the point reactor kinetics equations with Newtonian temperature feedback effects. *Ann. Nucl. Energy* **38**, 2810–2817 (2011). <https://doi.org/10.1016/j.anucene.2011.08.021>
33. A.A. Nahla, Numerical treatment for the point reactor kinetics equations using theta method, eigenvalues and eigenvectors. *Prog. Nucl. Energy* **85**, 756–763 (2015). <https://doi.org/10.1016/j.pnucene.2015.09.008>
34. A. Patra, S.S. Ray, On the solution of the nonlinear fractional neutron point-kinetics equation with Newtonian temperature feedback reactivity. *Nucl. Technol.* **189**(1), 103–109 (2015). <https://doi.org/10.13182/NT13-148>